This article has been accepted for publication in a future issue of this journal, but has not been fully edited. Content may change prior to final publication. Citation information: DOI 10.1109/TIE.2014.2311414, IEEE Transactions on Industrial Electronics

Zero Oscillation and Irradiance Slope Tracking for Photovoltaic MPPT

Francisco Paz, *Student Member, IEEE,* Martin Ordonez, *Member, IEEE*

***Abstract*—Maximum Power Point Tracking (MPPT) strategies in Photovoltaic (PV) systems ensure efficient utilization of PV arrays. Among different strategies, the Perturb and Observe (P&O) algorithm has gained wide popularity due to its intuitive nature and simple implementation. However, such simplicity in P&O introduces two inherent issues, an artificial perturbation that creates losses in steady-state operation and a limited ability to track transients in changing environmental conditions. This paper develops and discusses in detail an MPPT algorithm with zero oscillation and slope tracking to address those technical challenges. The strategy combines three techniques to improve steady-state behavior and transient operation: 1) idle operation on the Maximum Power Point (MPP), 2) identification of the irradiance change through a natural perturbation and 3) a simple multi-level adaptive tracking step. Two key elements, which form the foundation of the proposed solution, are investigated: the suppression of the artificial perturb at the MPP and the indirect identification of irradiance change through a current-monitoring algorithm which acts as a natural perturbation. The Zero-oscillation, Adaptive step Perturb and Observe (ZA-P&O) strategy builds on these mechanisms to identify relevant information and produce efficiency gains. As a result, the combined techniques achieve superior overall performance while maintaining simplicity of implementation. Simulations and experimental results are provided to validate the proposed strategy and illustrate its behavior in steady and transient operation.**

***Index Terms*—Solar power generation, Maximum power point trackers (MPPT).**

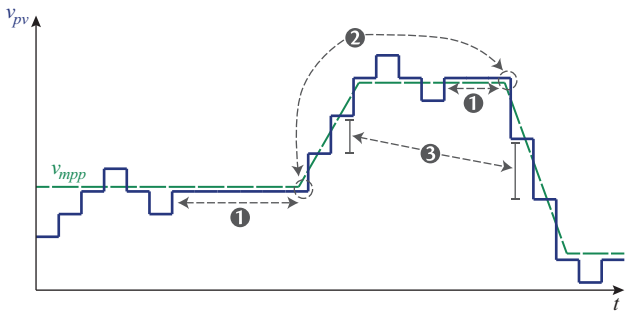

Fig. 1. Conceptual representation of the ZA-P&O combined MPPT strategies: efficiency maximized with no oscillation ❶, correct decision ❷ and step adjustment ❸ under changes in irradiance.

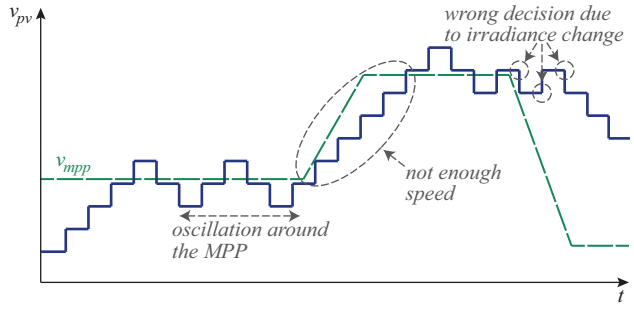

Fig. 2. Issues with P&O technique: oscillation in steady state, wrong tracking step and confusion during irradiance change.

I. Introduction

MAXIMUM Power Point Tracking (MPPT) for photovoltaic (PV) panels has seen many contributions in the past years [1] but some issues remain unsolved such as the oscillations in steady state, the tracking of changing environmental conditions and the global maximum location. Many techniques have been presented to track the Maximum Power Point (MPP) [2]–[8]; some have a very simple implementation but reduced efficiency, such as the Constant Voltage (CV), Fractional Open-Circuit Voltage (FOCV) and Fractional Short-Circuit Current (FSCI) methods, where the relationship between the open-circuit voltage/short-circuit current and the MPP voltage/current is assumed to be constant and independent of the environmental conditions [3].This techniques have been successfully implemented in extremely low power circuits like [9] and [10] boosting the energy harvested for autonomous equipment. Complex implementations achieve high performance by using a detailed model of the PV panel and additional measures of the irradiance (G) and temperature (T) [3], [11], [12].The use of G as a feed-forward variable produces precise results, at the expense of the use of an additional sensor.The hill-climbing techniques, Perturb and Observe (P&O) and Incremental Conductance (InCon), are simple algorithms that can obtain high efficiency with a low computational cost and with no information about the particular PV to which they are connected with a sufficient degree of reliability [13] and, for this reason, they have gained a predominant position amongst the MPPT algorithms. However, they both have similar issues regarding losses in steady-state [14], [15] and the identification and tracking of changing environmental conditions [16]–[19]. The Plane Division (PD) method [20] improves the speed of the standard InCon algorithm by creating a forbidden region, where the MPP cannot be located based on historical environmental data on the site and manufacturer information about the PV panel. A solution to the multiple maxima in the PV panel,

Manuscript received September 11, 2013; revised December 6, 2013 and February 6, 2014; accepted February 7, 2014

F. Paz and M. Ordonez are with the Department of Electrical and Computer Engineering, The University of British Columbia, Vancouver, BC, V6T 1Z4 Canada (phone: 1-604-827-1423; fax: 1-604-822-5949; e-mail: mordonez@ieee.org).

This article has been accepted for publication in a future issue of this journal, but has not been fully edited. Content may change prior to final publication. Citation information: DOI 10.1109/TIE.2014.2311414, IEEE Transactions on Industrial Electronics

due to mismatch, is addressed in [21], [22] by means of particle swarm optimization (PSO) and in [2], [4], [5], [23] by individually equalizing the differently irradiated cells. Other MPPT strategies are implemented using intelligent computations like Artificial Neural Networks [24] and Fuzzy logic [25]. Recent advancements using a Fuzzy-Neuro based algorithm, combined with an additional measurement G, obtain excellent precision in the tracking, but increasing the computational burden and cost.Finally, some applications allow for specific solutions that make use of the characteristics of the power converter [26], [27], such as the One Cycle Control in [6]–[8] for Grid connected systems.

Recently, some strategies have been developed to overcome the confusion that results from changes in G [28], [29]. Opportunities to further improve steady-state behavior and provide an accurate tracking under changing G exist and are explored in this work.

In this paper, the theory for a MPPT strategy referred to as Zero-oscillation, Adaptive-step Perturb and Observe (ZA-P&O) [30], which reduces losses in steady-state and improves tracking under speed-varying changes in G is developed. The losses are reduced by suppressing the artificial perturbation around the MPP in steady-state, and are made possible by indirectly estimating a change in G through the natural perturbation introduced by the error on a Proportional-Integral (PI) controller and the change in current in the operating point. Estimating the change enables the perturbation step to be adjusted in order to accurately track the changes in the MPP. The main advantages of this combined strategy are conceptually presented in Fig. 1 and compared with the standard P&O in Fig. 2. The improvements of the proposed strategy are summarized as follows: ❶ the efficiency in steady state is improved by suppressing the oscillation, ❷ the confusion caused by a change in G is eliminated and ❸ the step is adjusted for accurate tracking.

II. PV System Model

The block diagram of the implemented system is presented in Fig. 3. It includes a PV panel supplying energy through a power converter to a load, formed by a battery bank. The batteries are assumed to be discharged, and therefore able to absorb all the available power without influencing the MPPT process. The PV panel voltage and current (v_{pv},i_{pv}) are regulated by the controller to achieve the maximum power extraction determined by the ZA-P&O MPPT strategy. The DC/DC converter has a boost topology that ensures continuous current from the PV panel, minimizing the losses due to the current ripple.

In this section the model of the PV panel is presented. A summary of the basic P&O and its limitations is discussed. The losses due to the inaccuracy of MPPT are derived, showing the need to develop an improved MPPT strategy that minimizes the losses in steady state and boosts the accuracy of the tracking under changing environmental conditions. Finally, the concepts behind the implemented control loops are presented, introducing the natural perturbation concept that allows the elimination of the steady state oscillations and and enables

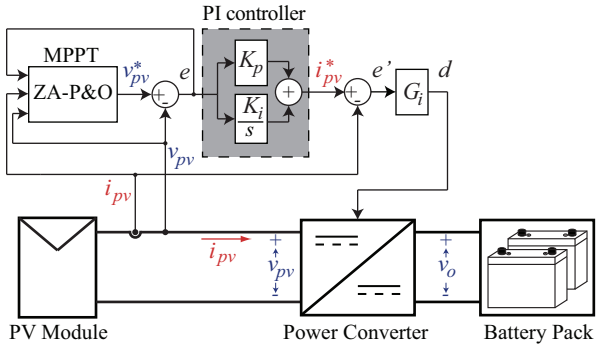

Fig. 3. Block diagram of the PV system, the PV panel is connected to a battery bank through a DC/DC power converter, the control system regulates the PV voltage to match the instructions of the MPPT block.

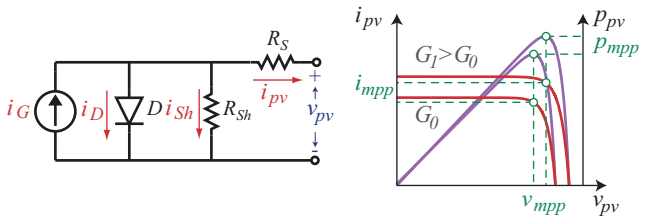

(a) (b)

Fig. 4. In (a) the Photovoltaic (PV) cell model including the parasitic effects of the series resistor (R_s) and the shunt resistor (R_{sh}), the photocurrent (i_G) is proportional to the irradiance (G); in (b) the characteristic I-V and P-V curves of the cell.

the dynamic adjustment of the step size in proportion to the change in G. The proposed ZA-P&O strategy builds on this foundation.

A. PV panel background

The equivalent circuit for a PV cell is presented in Fig. 4(a), including the effects of the series resistor (R_s) and the shunt resistor (R_{sh}). The diode D is characteristic of the P-N junction of the cell structure, while the photocurrent (i_G) is produced by the light photons arriving at the junction. The basic PV panel equations are reviewed to provide a clear background for the estimation of losses due to the MPPT strategy operation. For a PV panel built with M parallel strings of N cells connected in series, the panel's current (i_{pv}) at any given voltage (v_{pv}), temperature (T) and irradiance (G), neglecting the resistors, is given by

$$i_{pv} = Mi_G - MI_0\left(\exp\left(\frac{v_{pv}}{NnkT/q}\right) - 1\right). \quad (1)$$

where I_0 is the reverse saturation current of D, q is the electron charge, n is the diode factor, k is Boltzmann's constant (in joules per kelvin), T is the PV panel temperature (in kelvin) and i_G is proportional to G

$$i_G = \gamma G. \quad (2)$$

This relationship determines the influence of the environment variables (G,T) in the nonlinear cell characteristics and

This article has been accepted for publication in a future issue of this journal, but has not been fully edited. Content may change prior to final publication. Citation information: DOI 10.1109/TIE.2014.2311414, IEEE Transactions on Industrial Electronics

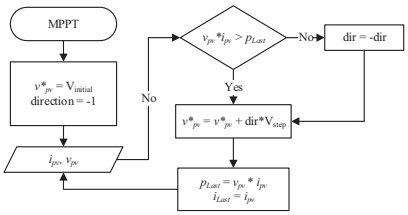

Fig. 5. Flowchart of the basic P&O MPPT algorithm.

is fundamental to develop a MPPT strategy that can track this changes. Two other basic magnitudes are of special interest when describing a PV cell and will be used to quantify the MPPT strategy behavior: the open-circuit voltage (V_{oc}) and the short-circuit current (I_{sc}). The V_{oc} is defined as v_{pv} when i_{sc} is null:

$$\begin{aligned} V_{oc} &= v_{pv}|_{i_{pv}=0} \\ &= \frac{NnkT}{q} \ln\left(\frac{i_G}{I_0} + 1\right). \end{aligned} \tag{3}$$

On the other hand, I_{sc} is defined as the i_{pv} when v_{pv} is null:

$$\begin{aligned} I_{sc} &= i_{pv}|_{v_{pv}=0} \\ &= M i_G. \end{aligned} \tag{4}$$

The characteristic I-V and P-V curves for a PV cell are shown in Fig. 4(b), the operating condition (v_{mpp},i_{mpp}) that yields the maximum available power (p_{mpp}) is called the Maximum Power Point (MPP). When the environmental conditions (G, T) change, the characteristic curves of the PV panel change and the MPP moves. The MPPT algorithm must not only be able to find the MPP in stationary environmental conditions, but to track it while it changes.

Both the change in G and in T influence the characteristics of the PV panel, but they do so in different ways. From the basic expressions (1)-(4) each influence can be quantified and studied. A change in G mostly affects I_{sc}, which increases proportionally to G, while V_{oc} remains almost the same as in Fig. 4(b) (for example, doubling G increases I_{sc} by 100% while V_{oc} only increases by 3%). On the other hand, changes in T mostly affect V_{oc} while I_{sc} is less affected (for example 1 K variation increases I_{sc} by 0.06% and V_{oc} is decreased by 0.4%). However, large gradients are expected from G due to clouding and shades, while T is expected to have a smaller gradient. The present work will focus only on the change in G with different dynamics (fast and slow) during the transient.

B. Basic P&O Algorithm Background

The flowchart of the basic P&O MPPT algorithm is presented in Fig. 5. The basic P&O scans the P-V curve of the panel in search for the MPP by changing the operating point (v^*_{pv} or i^*_{pv}), which is known as perturbation step, and then measuring the change in P (ΔP), known as observation step. If ΔP is greater than zero, then a new perturbation is introduced in the same direction. If ΔP is lower than zero, the direction of the perturbation is changed. The P&O keeps searching for the MPP until it has found an operating point such that ΔP is lower than zero in any direction; this condition is called steady-state. The P&O keeps perturbing the system in order to detect a change in the MPP (caused by a change in the environmental conditions), which triggers a new scan. An illustration of this process can be observed in Fig. 2. This steady-state perturbation drifts the operating point away from the MPP; this introduces losses. In theory, this perturbation can be reduced, reduced in order to keep the detection feature but minimize power losses. However, such a small perturbation would require extremely precise sensors to measure the change in power. Therefore, the perturbation in steady state (if kept) has a minimum amplitude that depends on the sensors.

Every time there is a change in the environmental conditions, there is a change in the P at the established operating point that masks the change caused by the perturbation. In this condition, the P&O algorithm might be induced to respond as though the perturbation introduced produced an effect different than the true one. As observed in Fig. 2, during the transient on the right (MPP moves to a lower voltage), since G is reduced, the overall P is reduced, regardless of the direction of the perturbation. In this condition, the P&O algorithm changes direction in each step, trapping the system until the transient finishes.

Finally, the classic P&O algorithm has a fixed step size, and therefore can only accurately track the change in the MPP when it moves at a given rate (providing it made the decision for the correct direction). The quantification of these losses is estimated in this paper.

The above mentioned issues present serious drawbacks to the P&O algorithm; the ZA-P&O MPPT tackles those limitations, as will be explained in Section III.

C. Steady-State Power Losses Estimation

The proposed MPPT strategy removes the oscillation around the MPP in steady state that is introduced by the artificial perturbation, and adapts the steps during a transient to accurately track the MPP in order to reduce the available power lost. A typical operation situation of a PV panel is displayed in Fig. 6, including a period in which G remains constant and a transient. The power losses in different stages of the MPPT (steady state or transient) are given by different expressions.

The power losses (P_r) in relationship with the available power (P_{mpp}) in steady state for the MPPT algorithms can be estimated as [14]

$$\frac{P_r}{P_{mpp}} \approx \left(\frac{(\Delta v_{pv})_{RMS}}{v_{mpp}}\right)^2 \left(1 + \frac{v_{cell}}{2nkT/q}\right), \tag{5}$$

where $(\Delta v_{pv})_{RMS}$ is the RMS value of the voltage oscillation and v_{cell} is the MPP voltage of each cell in the panel (around 0.5 V). As shown in the following equations, derived as part of this paper, (5) can be manipulated to compare the losses in steady state for the traditional P&O with the ZA-P&O. A cycle of the voltage oscillation around the MPP for the P&O is given by

This article has been accepted for publication in a future issue of this journal, but has not been fully edited. Content may change prior to final publication. Citation information: DOI 10.1109/TIE.2014.2311414, IEEE Transactions on Industrial Electronics

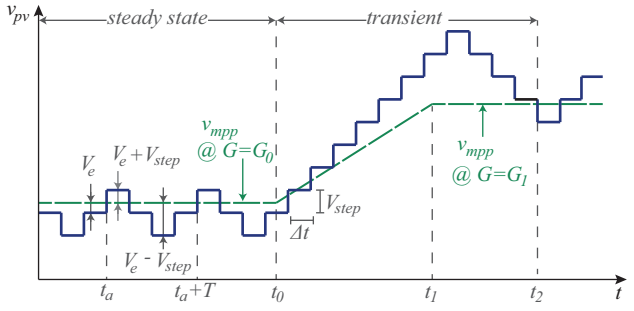

Fig. 6. The tracking losses depend on the different operating conditions (steady state or irradiance change).

$$\Delta v_{pv}(t) = \begin{cases} V_e + V_{step} & \text{if } 0 < t \leq T/4 \\ V_e & \text{if } T/4 < t \leq T/2 \\ V_e - V_{step} & \text{if } T/2 < t \leq 3T/4 \\ V_e & \text{if } 3T/4 < t \leq T, \end{cases} \tag{6}$$

where V_e is the difference between V_{mpp} and the closest v_{pv} set by the MPP tracker, due to the step size (see Fig. 6, in steady state). As can be observed, V_e is related to V_{step} by

$$V_e = bV_{step}, \tag{7}$$

where b is a number between -0.5 and 0.5. Therefore (6) can be expressed as

$$\Delta v_{pv}(t) = \begin{cases} (b+1)V_{step} & \text{if } 0 < t \leq T/4 \\ bV_{step} & \text{if } T/4 < t \leq T/2 \\ (b-1)V_{step} & \text{if } T/2 < t \leq 3T/4 \\ bV_{step} & \text{if } 3T/4 < t \leq T. \end{cases} \tag{8}$$

The RMS value of the voltage oscillation for the P&O is

$$\begin{aligned} (\Delta v_{pv})^{P\&O}_{RMS} &= \sqrt{\frac{1}{T}\int_0^T \Delta v(t)^2 dt} \\ &= V_{step}\sqrt{\frac{1}{4}((b+1)^2 + 2b^2 + (b-1)^2)} \\ &= V_{step}\sqrt{\frac{1}{2} + b^2}. \end{aligned} \tag{9}$$

If the voltage is kept as close as possible to the MPP (no oscillation), the RMS value of the voltage is

$$(\Delta v_{pv})^0_{RMS} = bV_{step}. \tag{10}$$

Replacing (9) in (5) gives the relative losses for the P&O algorithm in steady state

$$\left(\frac{P_r}{P_{mpp}}\right)_{P\&O} \approx \left(\frac{1}{2} + b^2\right)\left(\frac{V_{step}}{v_{mpp}}\right)^2\left(1 + \frac{v_{cell}}{2nkT/q}\right). \tag{11}$$

Replacing (10) in (5) gives the relative losses when the algorithm does not oscillate.

$$\left(\frac{P_r}{P_{mpp}}\right)_0 \approx b^2\left(\frac{V_{step}}{v_{mpp}}\right)^2\left(1 + \frac{v_{cell}}{2nkT/q}\right). \tag{12}$$

The ratio between (11) and (12) indicates the extra power lost by keeping the oscillation in steady state

$$\frac{(P_r/P_{mpp})_0}{(P_r/P_{mpp})_{P\&O}} \approx \frac{1/2 + b^2}{b^2} = 1 + \frac{1}{2b^2}. \tag{13}$$

As just demonstrated, (13) indicates that the losses in steady state are incremented by $1/2b^2$ because of the oscillation. In the best case, with $b = 0.5$, the losses are three times larger if the oscillation is maintained.

For a PV panel with $V_{oc} = 200$ V and $I_{sc} = 1$ A, v_{mpp} is around 170 V, the cell voltage at the MPP is around 0.5 V and with $V_{step} = 2$ V (1% of V_{oc}). The relative losses (expressed in percentage) using the $P\&O$ are obtained evaluating (11) for these specific values

$$\left(\frac{P_r}{P_{mpp}}\right)_{P\&O} \approx 0.09\%. \tag{14}$$

That means the oscillation around the MPP causes a 0.09% power losses. For the same PV panel, if the oscillation is removed in steady state, the losses and can be estimated as

$$\left(\frac{P_r}{P_{mpp}}\right)_0 \approx 0.03\%. \tag{15}$$

This configuration losses only 0.03% of the available power, three times less than does the traditional P&O. Projected in a 25 years life cycle of the PV setup this means a tangible benefit in overall energy production.

D. Irradiance Transient Power Losses Estimation

The following equations are derived in this work to quantify the losses due to dynamic MPPT error. During a transient in G, the MPP will move. The standard P&O algorithm has a fixed V_{step} and sampling time Δt; therefore it is able to accurately track only one slope of G, as seen in Fig. 6. If G changes more rapidly, the tracking would be inaccurate during the transient and would have to reach the MPP after the ramp stops. If G changes more slowly, the operating point would drift away from the MPP until the ramp stops, after which it would have to reach the true MPP (see Fig. 6).

During a ramp change in G from G_0 at t_0 to G_1 at t_1, G can be expressed as

$$G(t) = \begin{cases} G_0 & \text{if } t \leq t_0 \\ G_0 + (t - t_0)\delta G & \text{if } t_0 < t \leq t_1 \\ G_1 & \text{if } t_1 < t. \end{cases} \tag{16}$$

Then, the power extracted from the PV panel during the transient is given by

$$p_{pv}(t) = v_{pv}(t)\left(\gamma G(t) - I_0\left(\exp\left(\frac{v_{pv}(t)}{nkT/q}\right) - 1\right)\right). \tag{17}$$

A comparison with the maximum power (obtained while operating constantly at v_{mpp})

This article has been accepted for publication in a future issue of this journal, but has not been fully edited. Content may change prior to final publication. Citation information: DOI 10.1109/TIE.2014.2311414, IEEE Transactions on Industrial Electronics

$$p_{mpp}(t) = v_{mpp}(t)\left(\gamma G(t) - I_0\left(\exp\left(\frac{v_{mpp}(t)}{nkT/q}\right) - 1\right)\right), \tag{18}$$

shows the loss due to inaccurate tracking. The instantaneous tracking efficiency is given by

$$\eta_{MPPT}(t) = \frac{p_{pv}(t)}{p_{mpp}(t)}, \tag{19}$$

however, sometimes it is more important to have a more general overview of the losses. Computing the energy obtained through the transient (E_{pv}) and comparing it with the energy that would be obtained if the panel had always operated at the MPP (E_{mpp}) , enables the average tracking efficiency ($\bar{\eta}_{MPPT}$) to be quantified

$$\bar{\eta}_{MPPT} = \frac{E_{pv}}{E_{mpp}} = \frac{\int_{t_0}^{t_2} p_{pv}(t)dt}{\int_{t_0}^{t_2} p_{mpp}(t)dt}. \tag{20}$$

Numerically integrating these expression for a given PV panel using a P&O with a fixed Δt and V_{step} shows how $\bar{\eta}_{MPPT}$ is minimal for a certain δG.

These equations derived in this work provide valuable insight into the transient losses. The results for the example PV panel when G is changing from $G_0 = 600$ Wm^{-2} to $G_1 = 1000$ Wm^{-2} with several different δG are displayed in Fig. 7. The small sketches in Fig. 7 illustrate the tracking process with different slopes of G and a fixed step size: when the slope is slower than the steps, the tracking point overshoots; when the slope is higher than the steps, the tracking point takes time to catch up. There is one slope where the tracking point closely follows MPP. The power losses are minimal for a slope of 300 Wm^{-2}s^{-1}; this is the slope that the P&O can accurately track. If the slope is lower than the optimal, for example $\delta G = 100$ Wm^{-2}s^{-1}, v_{pv} will become larger than v_{mpp} leading to larger losses in the order of 3% (since the PV curves steeper for higher voltages as seen in Fig. 4(b)). When the slope is higher and the MPPT lags behind, for example for $\delta G = 600$ Wm^{-2}s^{-1}, the losses are around 0.1%. It is clear that a MPPT strategy that has a fixed step for tracking is not optimal during transients, and an adaptive strategy will ensure a closer tracking of the MPP in this condition, independent of the change in G.

E. Control System

Unlike most power converters, where the controller aims to regulate the output voltage, for MPPT purposes the controller regulates the input of the converter (v_{pv}). The controller is shown in Fig. 3. It uses a dual loop to regulate both i_{pv} and v_{pv}, this is then used to obtain additional information regarding the change in environmental conditions, a natural perturbation to the system. The inner loop (faster) will regulate i_{pv} by setting the duty cycle (d) of the converters switches. The outer loop, slower regulates v_{pv} to the level determined by the MPPT strategy (v_{pv}^*) by setting the reference current (i_{pv}^*).

The use of a dual-loop controller serves two purposes. On the one hand, it improves the stability of the system. On the other hand, it helps isolate the change in G acting as a natural perturbation to lead the MPPT. This avoids the use of a continuous artificial perturbation in steady state to track this change.

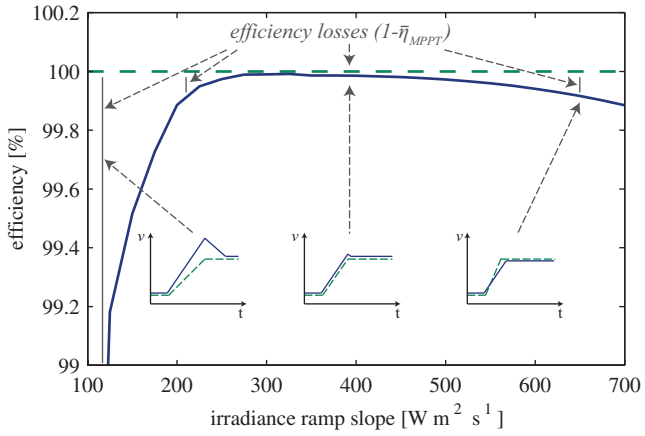

Fig. 7. Tracking efficiency ($\bar{\eta}_{MPPT}$) for a transient between $G_0 = 600$ Wm^{-2} to $G_1 = 1000$ Wm^{-2}, for a P&O algorithm with $\Delta t = 1$ s and $V_{step} = 2$ V showing the losses when the MPPT slope does not match the slope produced by δG.

Since v_{pv}^* is updated at the sampling speed of the MPPT (slower than the control system), during a sudden change in G, the outer loop will keep v_{pv} constant by changing i_{pv}. This change in i_{pv} indicates the change in G and acts as a natural perturbation. Moreover, it is shown in [29] that when G changes with a slope δG during the sample period (Δt) and the voltage loop has a PI controller the tracking error (e) is proportional to δG

$$e \propto \frac{\delta G}{K_i}. \tag{21}$$

Using this information, the proposed MPPT strategy can stop the artificial perturbation in steady state and monitor the change in i_{pv} and e (natural perturbation) to determine the change in the environment and adjust the step size (V_{step}).

III. Proposed MPPT Strategy

Now that the losses in steady-state and transient operation have been identified, the ZA-P&O MPPT strategy is developed based on two key aspects: 1) detection of the steady-state operation and 2) determination of the direction and magnitude of the perturbation. In steady-state, the standard P&O algorithm will oscillate around the closest possible voltage (due to quantization of the voltage step) in three levels, as in Fig. 2. This introduction of an artificial perturbation allows the MPPT to scan the curve for a change in the characteristics caused by environmental conditions. The ZA-P&O identifies this situation and establishes the operating point (v_{pv}^*) in the closest value, as shown in Fig. 1. In this operating mode, called idle mode, the losses are minimized as shown in section II-C. The environmental change is identified by monitoring the error in the PI controller (e) and the change in current (i_{pv}), which generate a natural perturbation clearly correlated to the change in the conditions.

This article has been accepted for publication in a future issue of this journal, but has not been fully edited. Content may change prior to final publication. Citation information: DOI 10.1109/TIE.2014.2311414, IEEE Transactions on Industrial Electronics

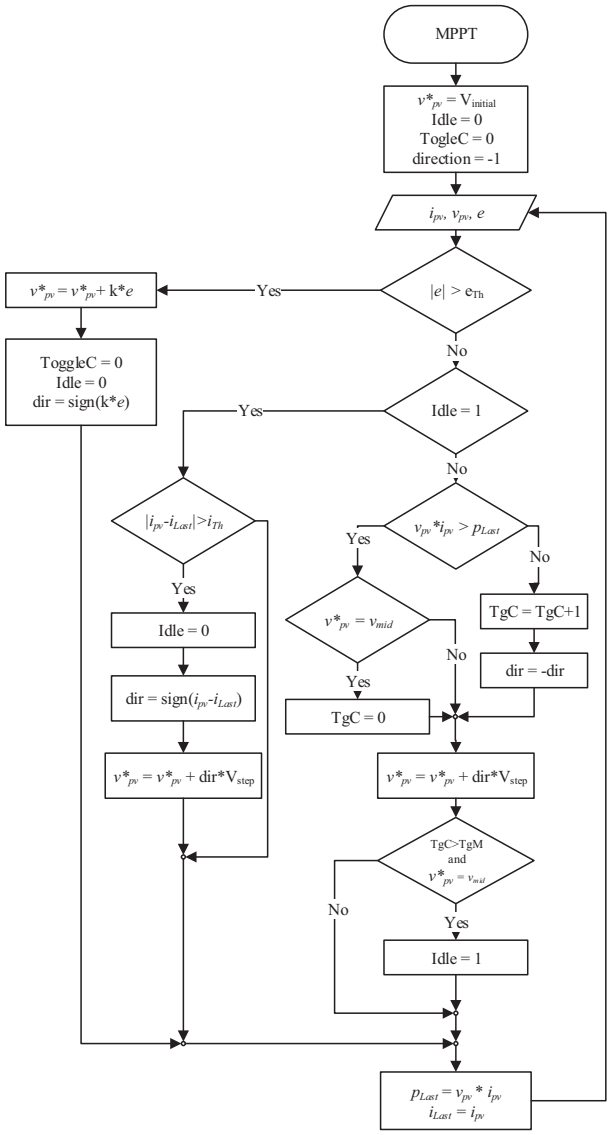

Fig. 8. Flow Chart for the ZA-P&O MPPT strategy.

The use of this natural perturbation enables a cleaner operation, removing redundant oscillations that are convoluted with the information of environmental change and can cause confusion. This allows tracking to reactivate when necessary and to establish an accurate step size based on the known slope, instead of toggling continuously as is usually done.

The flow chart for the ZA-P&O is presented in Fig. 8. The strategy includes tunable parameters, such as the thresholds for the current change and error (i_{Th} and e_{Th}) and the number of toggles around the MPP required to establish the idle mode (TgM). Outside the special conditions established before, the algorithm works as a P&O. In the following paragraphs, details regarding the implementation of the different features are given.

A. Idle mode operation

Conventional MPPT strategies search for the MPP by periodically changing v_{pv} and measuring the effect over p_{pv} or some other parameter. Since no way of identifying a change in G (and the corresponding displacement of the MPP) is included in the MPPT strategies, it must keep perturbing the operating point even when the MPP has been found (steady-state). This is reflected in a three-level operating condition shown in Fig. 2, where the operating point toggles around the closest voltage allowed by the discrete steps. This is an artificial perturbation that reduces the efficiency of the energy extraction.

The ZA-P&O MPPT strategy uses a natural perturbation, native to the control of the system, the change in i_{pv} and the error in the PI controller (with constant v^*_{pv}), making it possible to eliminate this perturbation. The proposed method identifies the operation in steady state by counting consecutive changes in direction with a common middle point (v_{mid}). When a step is introduced in v^*_{pv}, if the step is the second in the same direction, the algorithm displaces v_{mid}. The software computes one toggle and registers it in the toggle counter (TgC) each time the set point returns to v_{mid}. The maximum number of toggles around v_{mid} before activating the idled mode and removing the perturbation is set as a parameter (TgM) and is used to avoid confusion caused by noise.

B. Perturbation Direction and Magnitude Estimation

As explained in section II-E, the implemented controller can be used to monitor the changes in the environmental conditions. This leads to accurate knowledge of the magnitude of the change in G and the slope δG. This can be directly correlated to the displacement of v_{mpp} and i_{mpp}. This information provides the correct direction to the ZA-P&O.

In case of a slope change in G it is not enough to know the direction of the displacement. If the slope is too small, the MPPT may detect the change and introduce a step that will lead the operating point far away from the MPP. If the slope is too steep, the steps may not be large enough to track the MPP. Since the magnitude of the slope can be identified from (21), the magnitude of the change in i_{pv} that results from the change in G is known as

$$\Delta i_{pv} = K_i e \Delta t \tag{22}$$

where Δt is the sample time of the MPPT strategy. As can be seen, from the measurement of e and the knowledge of K_i and Δt, it is possible to know the change in i_{pv}, proportional to the change in G. In this condition, we can adjust the step in proportion to the change in the G. The value of the proportionality constant depends on the PV panel.

IV. Simulations

The results of the computer simulation for both the ZA-P&O MPPT and the standard P&O for a trapezoidal irradiance (G) profile are presented in this section. The model consists of a PV panel that can be configured to perform with the desired characteristics, a PI controller to regulate the voltage of the PV panel, and the MPPT to determine the operating point. The output of the PI controller sets the current in the PV panel.

The PV panel is configured to have 200 V open-circuit voltage and 5 A short-circuit current, with a Fill Factor (FF)

This article has been accepted for publication in a future issue of this journal, but has not been fully edited. Content may change prior to final publication. Citation information: DOI 10.1109/TIE.2014.2311414, IEEE Transactions on Industrial Electronics

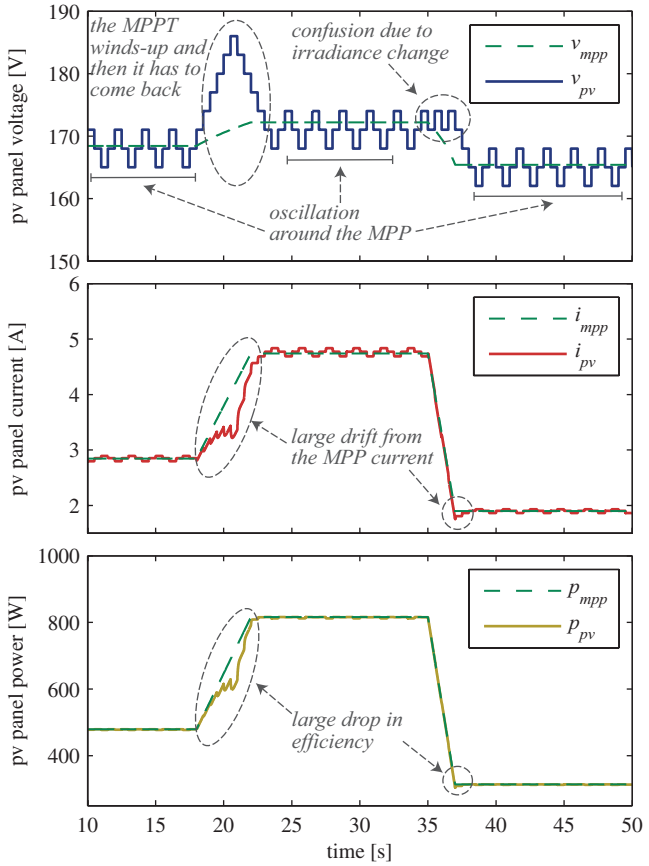

Fig. 9. Standard P&O issues when the irradiation (G) slope starts during a raising step of the algorithm for v_{pv}, i_{pv} and p_{pv}.

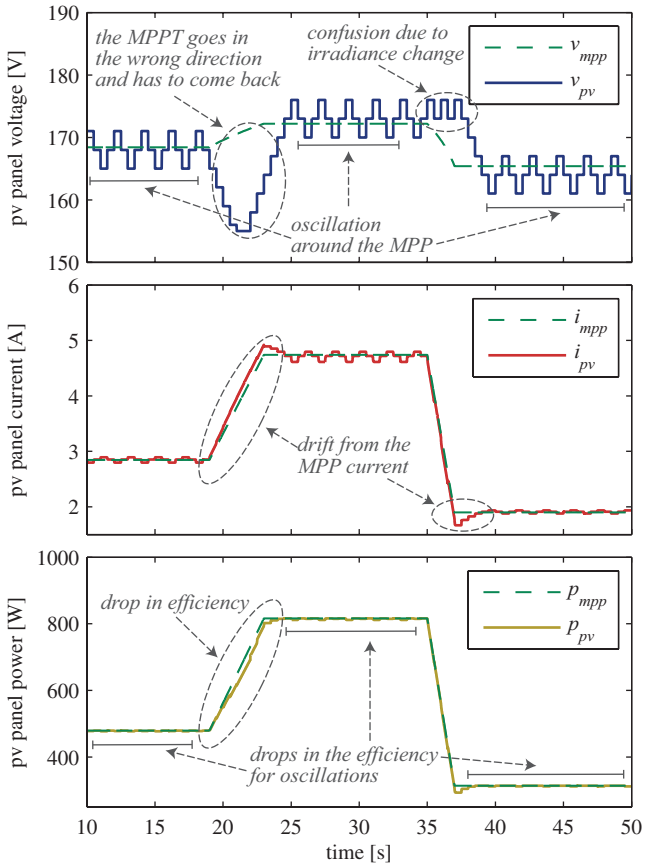

Fig. 10. Standard P&O issues when the irradiation (G) slope starts during a falling step of the algorithm for v_{pv}, i_{pv} and p_{pv}.

of 0.8 at standard test conditions (STC, 1 kW/m^2 and 25 °C). The MPPTs are configured with the same voltage step for the P&O part and the same sampling period. The sampling period of the MPPT is established in 0.5 s and the fixed voltage step is 3 V. The testing profile starts at 0.6 kW/m^2; at $t = 19$ s, it starts increasing with a slope of 0.1 kW/m^{2}s. When it reaches 1.0 kW/m^2, it stops and waits for 11 s and then it starts decreasing with a slope of 0.3 kW/m^{2}s until it reaches 0.4 kW/m^2. Then it remains constant until the end of the simulation. To illustrate the error in tracking for the standard P&O, two cases were studied, a) slope was started during a falling edge and b) during a raising edge of the MPPT. The input signals to the MPPT are v_{pv}, i_{pv} and the error of the PI controller. When the standard P&O is tested, the error is not used. For the simulations, the threshold level of the current and the error (i_{Th} and e_{Th}) are set to zero, since there is no noise in this environment.

The results of the simulation for the standard P&O are displayed in Figs. 9 and 10, while the results for the ZA-P&O MPPT are presented in Fig. 11. The standard P&O keeps going in the direction in which it was going when G changed (since it detects an increase in power) even when this direction is incorrect. When the irradiance decreases, it starts toggling in the same position, since any step produces a decrement in power. This deviation from the correct direction leads performance losses, since real profiles can have slopes for extended periods of time. Moreover, the standard MPPT algorithm is unable to adjust the tracking step to different δG; this leads to an algorithm that, even when it goes in the correct direction, may drift from the MPP because of the wrong step selection.

The ZA-P&O MPPT strategy resolves those issues effectively. The idle operating mode allows the PV panel to operate in a smooth way when there is no need to keep tracking. When a change occurs in G, the strategy clearly identifies the correct direction to move the operating point and adjusts the step size to provide a close tracking of the MPP. The effectiveness of the identification does not depend on the moment the irradiance slope starts.

The efficiency of the tracking for the three cases is shown in Fig. 12. It is evident that the ZA-P&O improves the overall performance: 1) in steady-state, the efficiency remains constant and close to 100% instead of oscillating periodically, 2) the correct direction is determined and 3) the step is adjusted; thus the efficiency remains high even during the transient, whereas the standard P&O leads to drops in efficiency.

For the V-I plane, Fig. 13 shows the trajectory of the tracking process for the P&O and for the ZA-P&O. The P&O deviates from the optimal trajectory, while the proposed strategy keeps very close track of it.

This article has been accepted for publication in a future issue of this journal, but has not been fully edited. Content may change prior to final publication. Citation information: DOI 10.1109/TIE.2014.2311414, IEEE Transactions on Industrial Electronics

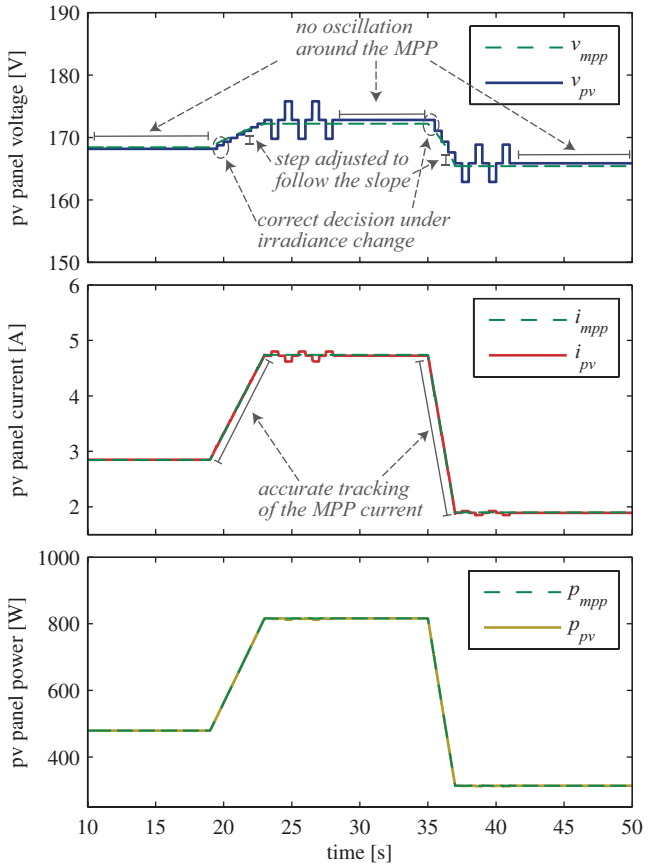

Fig. 11. ZA-P&O MPPT strategy improvements in steady state and transient for the voltage v_{pv}, i_{pv} and p_{pv}.

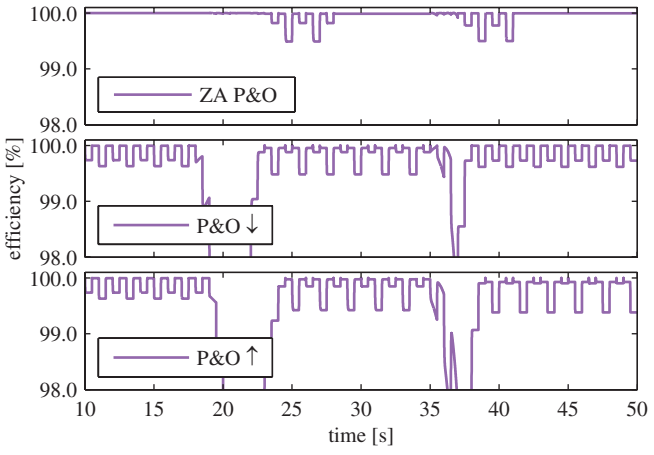

Fig. 12. Efficiency of the PV panel for the ZA-P&O and the standard P&O when the slope starts in the falling edge (P&O ↓) and in the raising edge (P&O ↑).

V. Experimental Results

The experimental setup of Fig. 14 was developed with the same parameters than the simulation to validate the ZA-P&O MPPT strategy. The prototype was implemented using an industry-standard microcontroller (TI C2000 core) typically employed to control power converters. The experimental results are shown in Figs. 15 and 16 for the standard P&O when

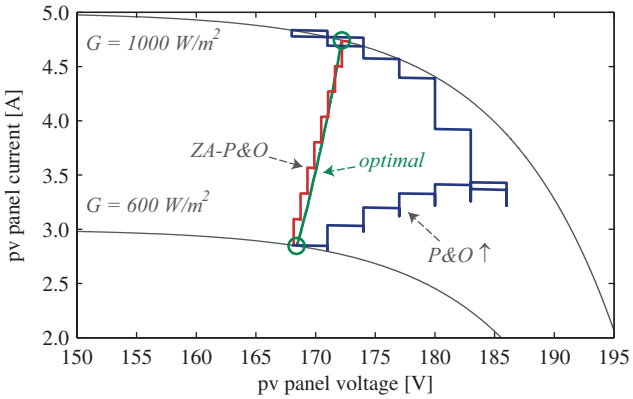

Fig. 13. P&O undesirable drifting behavior versus ZA-P&O direct trajectory in the V-I plane. The proposed strategy closely follows the locus of MPP.

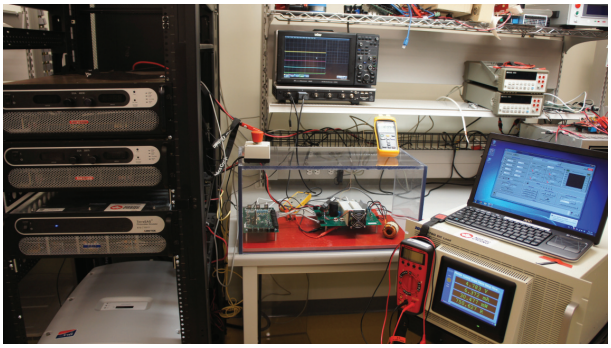

Fig. 14. Picture of the experimental setup.

the slope starts at a falling edge and a raising edge respectively and in Fig. 17 for the proposed strategy. The experimental captures closely match the simulation results. The experimental captures for the standard P&O (Figs. 15 and 16) show the characteristic issues: oscillation in steady state, wrong direction and wind-up. The benefits of the ZA-P&O are clearly shown in Fig. 17, when compared with the standard P&O. The oscillation is removed and the step is given in the correct direction and magnitude, as shown in the fast re-establishment of the idle mode after the irradiance slope ends. Calculating the total power produced during the transient for the three cases shows that the ZA-P&O produces 0.4% more energy comparing Fig. 17 and 16 and 0.7% more energy comparing Fig. 17 and 15. The overall efficiency of the ZA-P&O MPPT for this transients is 99.3%.

It can be seen in the experimental Figs. 15 and 16 that the standard P&O strategy drifts away from the MPP when G changes with a slope δG. Keeping the oscillation around the MPP in the idle condition increases the probability of making a mistake due to the noise in the measurement. This is demonstrated in Fig. 16, where the P&O process reaches the MPP during the first stage and works with three levels but suddenly drifts away and returns. The ZA-P&O algorithm benefits from the removal of this perturbation to enable a clearer measure of the change in G, which is represented by ❷ in Fig. 17.

This article has been accepted for publication in a future issue of this journal, but has not been fully edited. Content may change prior to final publication. Citation information: DOI 10.1109/TIE.2014.2311414, IEEE Transactions on Industrial Electronics

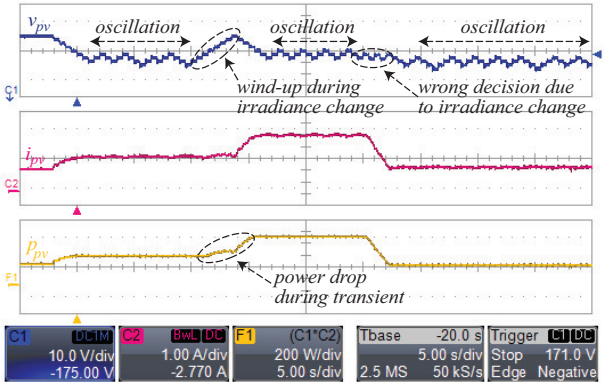

Fig. 15. Standard P&O experimental capture when the irradiance transient starts in a raising edge of the MPPT showing the issues of steady state oscillations and inaccurate tracking of transients.

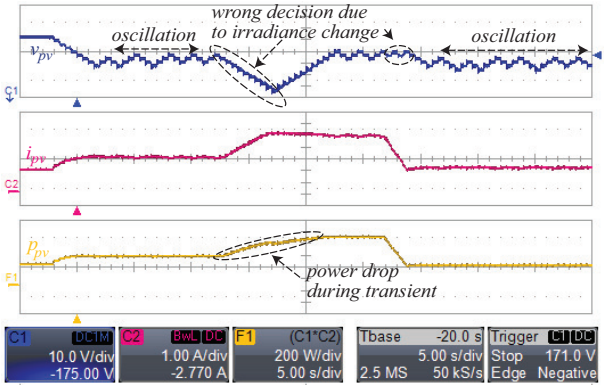

Fig. 16. Standard P&O experimental capture when the irradiance transient starts in a falling edge of the MPPT showing the issues of steady state oscillations and inaccurate tracking of transients.

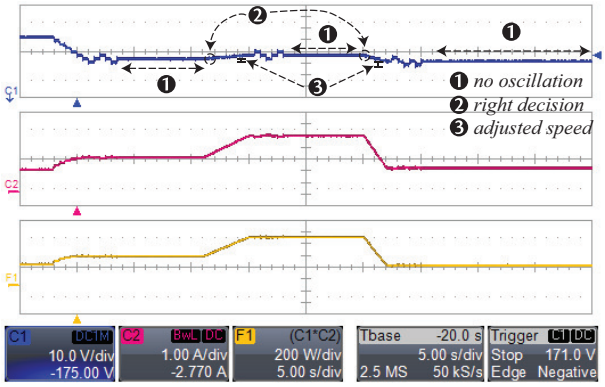

Fig. 17. ZA-P&O experimental test; the improvements are shown with the steady state operation and the accurate and fast tracking during transients.

The captures in Fig. 18 and Fig. 19 show the ZA-P&O MPPT for a different transient profile. The capture shows a detailed capture of the behavior, with a closer time scale and vertical scales. The experimental set shows how the ZA-P&O reacts to a very fast transient and a very slow one. As can be seen, the estimation of the new position ensures the correct direction and places the operating point close to the MPP in such a way that the local optimizations (activated after the transient) can locate the MPP in a few cycles and reactivate the Idle mode.

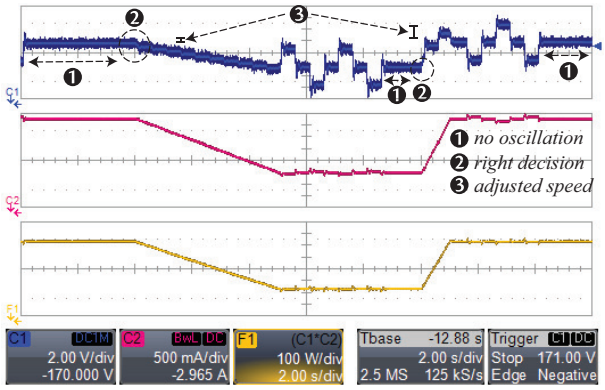

Fig. 18. ZA-P&O experimental test for a step down change from 1 kW m^{-2} to 500 W m^{-2} in 5 s and then back to 1 kW m^{-2} in 1 s.

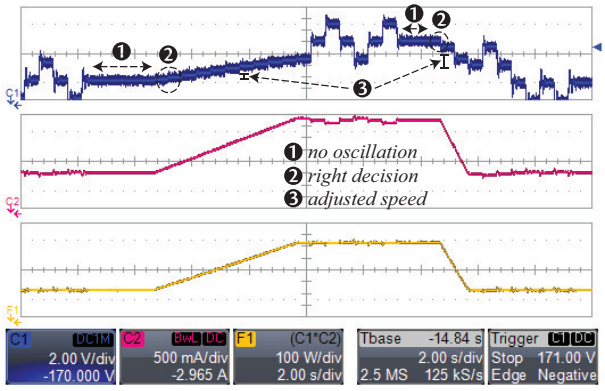

Fig. 19. ZA-P&O experimental test for a step up change from 500 W m^{-2} to 100 W m^{-2} in 5 s and then back to 500 W m^{-2} in 1 s.

VI. Conclusions

The Zero-oscillation, Adaptive-step Perturb and Observe (ZA-P&O) Maximum Power Point Tracking (MPPT) strategy for solar photovoltaic (PV) panels was presented in this work. This combined strategy reduced steady-state losses and improved transient behavior during slope changes irradiance, while maintaining a similar implementation complexity. Enhanced behavior resulted from the combination of three techniques: 1) idle operation when steady-state is reached, 2) correct irradiance change identification and 3) multi-level adaptive tracking step. The idle operation was possible due to the identification of the irradiance slope through a current monitoring algorithm. The adaptive tracking speed minimized error during a fast change in irradiance. The proposed combined techniques were studied with simulations and validated through experimental results implemented in a low cost microcontroller. The overall performance improvements, both in steady-state and during fast irradiance change show the benefits of the combined techniques.

References

[1] M. de Brito, L. Galotto, L. Sampaio, G. de Azevedo e Melo, and C. Canesin, "Evaluation of the main mppt techniques for photovoltaic

applications," *IEEE Trans. Ind. Electron.*, vol. 60, no. 3, pp. 1156 –1167, Mar. 2013.

[2] N. Femia, G. Lisi, G. Petrone, G. Spagnuolo, and M. Vitelli, "Distributed maximum power point tracking of photovoltaic arrays: Novel approach and system analysis," *IEEE Trans. Ind. Electron.*, vol. 55, no. 7, pp. 2610–2621, Jul. 2008.

[3] B. Subudhi and R. Pradhan, "A comparative study on maximum power point tracking techniques for photovoltaic power systems," *IEEE Trans. on Sustain. Energy*, vol. 4, no. 1, pp. 89 –98, jan. 2013.

[4] G. Adinolfi, N. Femia, G. Petrone, G. Spagnuolo, and M. Vitelli, "Energy efficiency effective design of dc/dc converters for dmppt pv applications," in *35th IEEE Annu. Conf. Industrial Electronics (IECON)*, Porto, Portugal, Nov. 2009, pp. 4566–4570.

[5] G. Petrone, G. Spagnuolo, and M. Vitelli, "An analog technique for distributed mppt pv applications," *IEEE Trans. Ind. Electron.*, vol. 59, no. 12, pp. 4713–4722, Dec. 2012.

[6] N. Femia, D. Granozio, G. Petrone, G. Spagnuolo, and M. Vitelli, "Optimized one-cycle control in photovoltaic grid connected applications," *IEEE Trans. Aerosp. Electron. Syst*, vol. 42, no. 3, pp. 954–972, Jul. 2006.

[7] M. Fortunato, A. Giustiniani, G. Petrone, G. Spagnuolo, and M. Vitelli, "Maximum power point tracking in a one-cycle-controlled single-stage photovoltaic inverter," *IEEE Trans. Ind. Electron.*, vol. 55, no. 7, pp. 2684–2693, Jul. 2008.

[8] E. Sreeraj, K. Chatterjee, and S. Bandyopadhyay, "One-cycle-controlled single-stage single-phase voltage-sensorless grid-connected pv system," *IEEE Trans. Ind. Electron.*, vol. 60, no. 3, pp. 1216–1224, Mar. 2013.

[9] O. Lopez-Lapena, M. Penella, and M. Gasulla, "A closed-loop maximum power point tracker for subwatt photovoltaic panels," *IEEE Trans. Ind. Electron.*, vol. 59, no. 3, pp. 1588–1596, Mar. 2012.

[10] A. Weddell, G. Merrett, and B. Al-Hashimi, "Photovoltaic sample-and-hold circuit enabling mppt indoors for low-power systems," *IEEE Trans. Circuits Syst. I, Reg. Papers*, vol. 59, no. 6, pp. 1196 –1204, Jun. 2012.

[11] J. Blanes, F. Toledo, S. Montero, and A. Garrigos, "In-site real-time photovoltaic i-v curves and maximum power point estimator," *IEEE Trans. Power Electron*, vol. 28, no. 3, pp. 1234 –1240, Mar. 2013.

[12] T. Esram and P. Chapman, "Comparison of photovoltaic array maximum power point tracking techniques," *IEEE Trans. Energy Convers.*, vol. 22, no. 2, pp. 439–449, Jun. 2007.

[13] G. Petrone, G. Spagnuolo, R. Teodorescu, M. Veerachary, and M. Vitelli, "Reliability issues in photovoltaic power processing systems," *IEEE Trans. Ind. Electron.*, vol. 55, no. 7, pp. 2569–2580, Jul. 2008.

[14] C. Sullivan, J. Awerbuch, and A. Latham, "Decrease in photovoltaic power output from ripple: Simple general calculation and the effect of partial shading," *IEEE Trans. Power Electron*, vol. 28, no. 2, pp. 740 –747, feb. 2013.

[15] R. Faranda, S. Leva, and V. Maugeri, "Mppt techniques for pv systems: Energetic and cost comparison," in *IEEE Power and Energy Society General Meeting - Conversion and Delivery of Electrical Energy in the 21st Century*, Pitsburg, PA, Jul. 2008, pp. 1–6.

[16] M. Elgendy, B. Zahawi, and D. Atkinson, "Assessment of the incremental conductance maximum power point tracking algorithm," *IEEE Trans. on Sustain. Energy*, vol. 4, no. 1, pp. 108 –117, jan. 2013.

[17] ——, "Assessment of perturb and observe mppt algorithm implementation techniques for pv pumping applications," *IEEE Trans. on Sustain. Energy*, vol. 3, no. 1, pp. 21 –33, jan. 2012.

[18] S. Kjaer, "Evaluation of the "hill climbing" and the "incremental conductance" maximum power point trackers for photovoltaic power systems," *IEEE Trans. Energy Convers.*, vol. 27, no. 4, pp. 922 –929, dec. 2012.

[19] M. Berrera, A. Dolara, R. Faranda, and S. Leva, "Experimental test of seven widely-adopted mppt algorithms," in *IEEE Bucharest PowerTech (BPT)*, Bucharest, Romania, Jun. 2009, pp. 1–8.

[20] H. Koizumi, "A summary of plane division maximum power point tracking methods," in *IEEE Int. Conf. on Sustainable Energy Technologies (ICSET)*, Singapore, Singapore, Nov. 2008, pp. 306–311.

[21] M. Miyatake, M. Veerachary, F. Toriumi, N. Fujii, and H. Ko, "Maximum power point tracking of multiple photovoltaic arrays: A pso approach," *IEEE Trans. Aerosp. Electron. Syst.*, vol. 47, no. 1, pp. 367–380, Jan. 2011.

[22] K. Ishaque and Z. Salam, "A deterministic particle swarm optimization maximum power point tracker for photovoltaic system under partial shading condition," *IEEE Trans. Ind. Electron.*, vol. 60, no. 8, pp. 3195–3206, Aug. 2013.

[23] L. Villa, T.-P. Ho, J.-C. Crebier, and B. Raison, "A power electronics equalizer application for partially shaded photovoltaic modules," *IEEE Trans. Ind. Electron.*, vol. 60, no. 3, pp. 1179–1190, Mar. 2013.

[24] L. Elobaid, A. Abdelsalam, and E. Zakzouk, "Artificial neural network based maximum power point tracking technique for pv systems," in *38th IEEE Annu. Conf. Industrial Electronics (IECON)*, Montreal, QC, Oct. 2012, pp. 937–942.

[25] B. Alajmi, K. Ahmed, S. Finney, and B. Williams, "A maximum power point tracking technique for partially shaded photovoltaic systems in microgrids," *IEEE Trans. Ind. Electron.*, vol. 60, no. 4, pp. 1596 –1606, Apr. 2013.

[26] M. Boztepe, F. Guinjoan, G. Velasco-Quesada, S. Silvestre, A. Chouder, and E. Karatepe, "Global mppt scheme for photovoltaic string inverters based on restricted voltage window search algorithm," *IEEE Trans. Ind. Electron.*, vol. 61, no. 7, pp. 3302–3312, Jul. 2014.

[27] E. Mamarelis, G. Petrone, and G. Spagnuolo, "Design of a sliding-mode-controlled sepic for pv mppt applications," *IEEE Trans. Ind. Electron.*, vol. 61, no. 7, pp. 3387–3398, Jul. 2014.

[28] D. Sera, R. Teodorescu, J. Hantschel, and M. Knoll, "Optimized maximum power point tracker for fast-changing environmental conditions," *IEEE Trans. Ind. Electron.*, vol. 55, no. 7, pp. 2629 –2637, Jul. 2008.

[29] R. Kadri, J.-P. Gaubert, and G. Champenois, "An improved maximum power point tracking for photovoltaic grid-connected inverter based on voltage-oriented control," *IEEE Trans. Ind. Electron.*, vol. 58, no. 1, pp. 66 –75, jan. 2011.

[30] F. Paz and M. Ordonez, "Zero-oscillation adaptive-step solar maximum power point tracking for rapid irradiance tracking and steady-state losses minimization," in *3rd IEEE Int. Symp. Power Electronics for Distributed Generation Systems (PEDG)*, Rorgers, AR, Jul. 2013.

Francisco Paz (S'08) was born in La Plata, Argentina. He received the Ing. degree in Electronics Engineering from the National University of Comahue, Neuquen, Argentina, in 2012. He began research activities during that year at the University of British Columbia in Vancouver, BC, Canada where he is currently working towards a M.A.Sc degree.

His current interests include renewable energy conversion, maximum power point tracking and renewable energy system topologies for solar, wind and marine power.

Mr. Paz was recognized with a scholarship from the Argentinian Ministry of Education and the Ministry of Science, Technology and Productive Innovation from 2008 to 2010.

Martin Ordonez (S'02-M'09) was born in Neuquen, Argentina. He received his Ing. degree in electronics engineering from the National Technological University, Argentina, in 2003 and his M.Eng. and Ph.D. degrees in electrical engineering from the Memorial University of Newfoundland, St. John's, NL, Canada, in 2006 and 2009, respectively.

Dr. Martin Ordonez is currently an Assistant Professor with the Department of Electrical and Computer Engineering at The University of British Columbia (UBC) in Vancouver, Canada. He is also an Adjunct Professor with Simon Fraser University (SFU) and Memorial University of Newfoundland (MUN). His industrial experience in Power Conversion includes research and development at Xantrex Technology Inc. / Elgar Electronics Corp. (now AMETEK Programmable Power), Deep-Ing Electronica de Potencia, and TRV Dispositivos, where he developed high-density dc-dc power converters, UPS inverters, and digital controllers.

Dr. Ordonez has an active research program in power conversion for renewable energy systems and has developed partnerships with various companies in the sector. With the support of industrial funds and the Natural Sciences and Engineering Research Council (NSERC), he has contributed more than 60 publications and R&D reports in the power area. He is an Associate Editor for IEEE TRANSACTIONS ON POWER ELECTRONICS, serves on several IEEE committees, and reviews widely for IEEE/IET journals and international conferences. He was awarded with the David Dunsiger Award for excellence in the Faculty of Engineering and Applied Science (2009), the Chancellors Graduate Award/Birks Graduate Medal (2006) and as a Fellow of the School of Graduate, Memorial University.